Journal of the European Ceramic Society 20 (2000) 1241–1250

Oxygen stoichiometry and mixed ionic-electronic conductivity of $Sr_{1-a}Ce_aFe_{1-b}Co_bO_{3-x}$ perovskite-type oxides

N.E. Trofimenko*, H. Ullmann

Institute of Inorganic Chemistry, Technical University Dresden, Mommenstr. 13, 01062 Dresden, Germany

Received 28 June 1999; received in revised form 21 October 1999; accepted 31 October 1999

Abstract

The structure, oxygen stoichiometry, total and ionic electrical conductivities of $Sr_{1-a}Ce_aFe_{1-b}Co_bO_{3-x}$ ($a=0\div0.2$, $b=0\div1.0$) were investigated. XRD patterns show the cubic perovskite structure of all air-treated samples. In reducing atmosphere the Co rich compositions were partially decomposed. The change of the lattice parameter a with Ce content could be explained on the basis of the oxygen stoichiometry values, determined by solid electrolyte investigations. The total conductivity (p-type, above 400–800°C changing to metallic-like behaviour) was enhanced by the Co content and reached 200 S cm^{-1} at 600°C. From permeation measurements an ionic conductivity higher than YSZ and for the compositions of lower ceria content as high as gadolinia doped ceria was observed. The results are compared with those of $La_{1-a}Sr_aFe_{1-b}Co_bO_{3-x}$ and of manganites.

Keywords: Electrical conductivity; Lattice parameter; Ionic conductivity; Perovskites; $(Sr,Ce)(Fe,Co)O_3$

1. Introduction

In search of electrode materials of enhanced electrocatalytic activity for SOFC perovskite oxides with higher oxygen transport became of great interest.[1] Higher defective and thermodynamically less stable oxides meet these requirements. $La_{1-a}Sr_aFe_{1-b}Co_bO_{3-x}$ was one of the most investigated alternative to the lanthanum strontium manganites within the III-III-perovskites. Most of the compositions cover the lanthanum-rich corner of the La–Sr–Fe–Co composition area. The consistency of the published results on their oxygen transport properties[2–10] may suffer from the different complicated experimental methods, and additionally from the way of calculation of the diffusion coefficients on the basis of experimental data. In some investigations the influence of dopands was overlapped by neglection of surface exchange limitation or structure changes. The tendencies within experimental sequences of individual authors are more convincing: Excluding some results,[3,4] an increase of ionic conductivity with A-site doping was observed, which increases the oxygen vacancy concentration.[2,5–10] Electronic conductivity is more influenced by B-site occupation, and it is nearly independent on A-site. Increasing Fe on B-site increased the E_a for oxide ion diffusion.[2,7]

The possibility of stabilization of the perovskite structure in the highly-defective II-III-perovskite oxides $SrCoO_{3-x}$ and $SrFeO_{3-x}$ by Ce^{4+}, which is inserted as demonstrated[11,12] on A-site enables the investigation the Sr-rich corner of the La–Sr–Fe–Co composition area. La is substituted by cerium with lower ionic radius and higher positive charge. The results for $Sr_{0.9}Ce_{0.1}CoO_{3-x}$[11,13,14] demonstrated highest electrical (500 S cm-1 at 400°C) and oxygen ionic conductivities (0.15 S cm^{-1} at 800°C) combined with highest oxygen deficiency. Because the cobaltite is decomposed at 600°C below 1 Pa of oxygen pressure, measures must be taken to stabilize this material without substantial loss in conductivity.

The partial substitution of Co by Fe ions in the composition $Sr_{1-a}Ce_aFe_{1-b}Co_bO_{3-x}$ ($a=0$–0.4, $b=0$–1.0) could be of interest for stabilization of the cobaltite. The limit of cerium solubility in $Sr_{1-a}Ce_aMeO_{3-x}$ (M = Co, Fe) to form the cubic perovskite structure was observed[11,12] at $a=0.15$. Small doping levels of cerium

* Corresponding author. Tel.: +39-251-463-4792; fax: +49-351-463-7752.

E-mail address: nikolai.trofimenko@chemie.tu-dresden.de (N.E. Trofimenko).

0955-2219/00/$ - see front matter
PII: S0955-2219(99)00292-7

in $Sr_{1-a}Ce_aFe_{1-b}Co_bO_{3-x}$ (up to a <0.03 mol) at $b=0$ and 1.0 result in a crystal structure similar to that of pure $SrFeO_{3-x}$ and $SrCoO_{3-x}$, respectively.[15] The ionic radius[16] of Ce^{4+} ($r=1.14$ Å) is smaller than that of Sr^{2+} ($r=1.44$ Å) and the attraction between cerium and oxygen ions is stronger than that between strontium and oxygen. The oxygen deficiency x and average valence state of B-site cation decrease with increasing ceria concentration. These facts should be arguments for a decreasing lattice parameter. The lattice parameters of the (pseudo)cubic perovskite lattice decrease in the case of cobaltite, but increase in the case of ferrate, as depicted in Fig. 1 (see in discussion).

The effect of strontium substitution by cerium and/or iron substitution by cobalt on structure and lattice parameters have to be evaluated in detail. The changes in structural and charge transport properties of this system should be understood on the basis of XRD data and experimental values of the oxygen deficiency x. The electronic and oxygen ionic transport was investigated in terms of dependency on composition and oxygen stoichiometry.

2. Fundamental

Doping and substitution within a certain structure require to keep the rules of geometrical and charge balance within the crystall. On this basis the relations between oxygen stoichiometry and oxidation state of the different cations can be estimated. In the compositions $Sr_{1-a}Ce_aFe_{1-b}Co_bO_{3-x}$ with tetravalent Ce^{4+} on the site of divalent Sr^{2+} electroneutrality requires the compensation of the effective positive charges of the cerium cations by a decrease in valence of some B-site cations (electronic compensation) and/or by the decrease of the concentration of oxygen vacancies (ionic compensation). As known for III-III-perovskite oxides both defect types B_B^{4+} and V_o^{**} exist.[17] Their concentrations will change with oxygen partial pressure, temperature, doping concentration on A-site and type of transition metal cation on B-site. Cerium doping decreases the concentration of V_O^{**} and simultaneously of Fe^{4+} evoking a corresponding increase in the average size of the B-place cations (ionic radii after[16]). For $a=0$–0.1 the oxidation states Fe^{3+} and Fe^{4+} are preferred, whereas increasing cerium concentration to $a>0.1$ requires the formation of Fe^{2+} in addition to Fe^{4+} ions within the perovskite structure. The relations in cobaltite will be similarly, but greater tendency to the formation of the 2+ oxidation state of Co in relation to Fe must be considered.[18]

In accordance with the Kröger-Vink notation the defect reactions for the reduction of air-treated samples are described as follows, for undoped samples (M = Fe or Co)

$$Sr_xM^x_{2x}M^*_{1-2x}O_{3-x}V^{**}_{O,x'} => Sr^xM^x_{2x'+2\delta}M^*_{1-2x'-2\delta}O_{3-x-\delta}V^{**}_{O,x'+\delta} + \delta/2O_2 \quad (1)$$

for Ce-doped samples

$$Sr^x_{1-a}Ce^{**}_aM^x_{2x'+2a'}M^*_{1-2x'-2a'}O_{3-x'+a-a'}V^{**}_{O,x'-a+a'} => Sr^x_{1-a}Ce^{**}_aM^x_{2x'+2a'+2\delta}M^*_{1-2x'-2a'-2\delta}O_{3-x'+a-a'-\delta}V^{**}_{O,x'-a+a'+\delta} + \delta/2O_2 \quad (2)$$

where $x = x' - a + a' + \delta$; $a = a' + (a - a')$, $Sr^{2+}(Sr^x)$ is written for a regular and Ce^{4+} (Ce^{**}) for a two fold overloaded A-site occupation and M^{3+} (M^x) for a regular and M^{4+} (M^*) as the one fold overloaded B-site occupation.

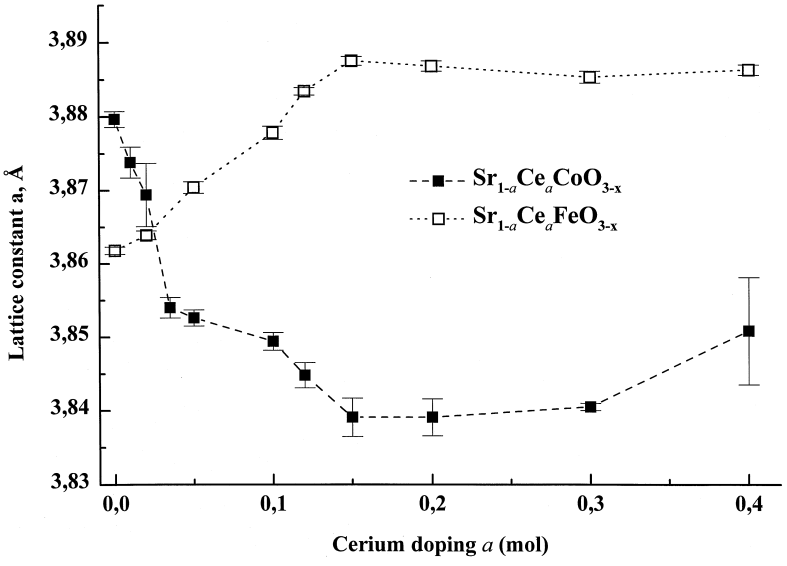

Fig. 1. Lattice parameter a of the cubic perovskite phases of strontium cobaltite and strontium ferrate, stabilized by cerium, after.[11,12]

It can be assumed, that in $Sr_{1-a}Ce_aMO_{3-x}$ (M = Co, Fe, a = 0–0.4) electronic/ionic compensation may be conditioned by the following mechanisms:

(a) reduction of M^{4+} cations ($M^{4+} \rightarrow M^{3+}$), which is prefered for $a < 0.1$,
(b) decrease of the concentration of V_O^{**}, which is expected, considering the tendency of cerium to suppress oxygen deficiency,[11,12]
(c) the reduction of M^{3+} to M^{2+} for $a \geqslant 0.1$, as reported for other perovskite systems too.[19–21]

Increasing substitution of Sr by Ce shifts the start of charge disproportionation below room temperature.[19]

3. Experimental procedure

3.1. Sample preparation

Samples of the composition $Sr_{1-a}Ce_aFe_{1-b}Co_bO_{3-x}$ (a = 0–0.4, b = 0–1.0) were prepared from $SrCO_3$, CeO_2, Fe_2O_3, Co_3O_4 of 99.9% purity. The compounds were mixed in a mortar, heated in air for 20 h at 1150°C. After cooling to room temperature the products were crushed and ground for 24 h. The powders were pressed into pellets in the absence of a binder and sintered in air at 1250–1350°C for 20 h.

X-ray diffractograms were obtained by means of a mono-chromated CuK_a radiation with a Siemens D5000 equipment. For determination of the lattice parameters aluminum was used as an internal standard. The averaged 2θ deviation for the Al standard was 0.045–0.060°. All air-treated samples were of cubic symmetry. No change in diffraction patterns were observed in samples quenched from 1000°C in argon.

Densities of the sintered samples were determined with a gas pycnometer, model AccuPyc-1330, from micrometrics. All relative densities were greater then 93% of theoretical, the samples were gas tight. Theoretical densities were estimated from the unit cell composition.

Oxygen deficiencies were measured by the solid electrolyte coulometric (SEC) device Oxylyt (SensoTech Magdeburg).[22] Samples of the powders are reacted in a temperature programmed furnace with a gas of controlled oxygen partial pressure. After reaction with the sample the deviation of the oxygen content from the initial state was determined by SEC titration. Gases of controlled oxygen partial pressures (investigated range: 10^{-10}–10^5 Pa) were prepared from argon/air or argon/hydrogen/water vapour mixtures, the P_{O2} values were modified within the oxidizing and reducing regions by subsequent electrolytic pumping. The P_{O2} values were measured by a solid electrolyte potentiometric cell.

The electrical conductivity was measured by a d.c. four-point method on sintered shapes of 3×2×10 mm size. The temperature range investigated was 20–1000 ± 2°C. During the measurements the oxygen partial pressure or temperature were kept constant.

Oxygen permeation was measured without an applied electrical field between 700 and 1000°C (temperature step method). The experimental technique was described in Ref. 13. The heating and cooling rates were 1°C/min), using sintered disks (10 mm diameter×1.0–2.0 mm thick) sealed with gold ring in an alumina tube. Two surfaces of the pellet were exposed to gas flows with different oxygen partial pressures, controlled by the Oxylyt. The permeation flux of oxygen from the high- to the low-pressure side was measured using the solid electrolyte technique. In all experiments air was used as the gas on the high P_{O2} side, and argon/O_2 mixtures (70–80 Pa) on the low P_{O2} side. The absence of mass transfer limitations was verified by variation of the total flow rate between 3 and 10 l/h at constant P_{O2} at the outlet of the reactor. Within experimental error no significant change of permeation was observed. At each temperature an equilibration time (1–3 h) was required before the permeation flux reached equilibrium. The lower the temperature and oxygen partial pressure, the longer the time for equilibration.

4. Results and discussion

4.1. Oxygen stoichiometry and lattice parameters

4.1.1. A-site doped strontium cobaltite and strontium ferrate

Doping with ceria leads to increasing oxygen stoichiometry ($3-x$). On the basis of experimental determined ($3-x$) values of the air treated samples (above 1000°C, followed by slow cooling) the concentrations of different oxidation states of the transition metal cations and from these the average B-site radii were calculated. The influence of cerium doping on the average size of B-site cations is shown in Fig. 2a and b. The decreasing lattice constant a of the cobaltite in the region $a < 0.15$ can be calculated from the assumption of Co^{3+} and Co^{4+} ions (average r = 0.60 Å) with increasing Ce content (Fig. 2a). The increase of the lattice constant in strontium ferrate relative to the cobaltite can only be explained by assumption of the more voluminous Fe^{2+} and Fe^{4+} ions (average r = 0.647 Å) (Fig. 2b).

4.1.2. B-site substitution of mixed cobaltite/ferrate

The dependence of the cubic lattice constant a on substitution of iron by cobalt at constant cerium content in $Sr_{0.9}Ce_{0.1}Fe_{1-b}Co_bO_{3-x}$ was investigated (Fig. 3). A good correlation between ionic radii and XRD data was observed. All samples were of cubic structure. With increasing Co content b the lattice constant a gradually decreases, connecting the values of the end

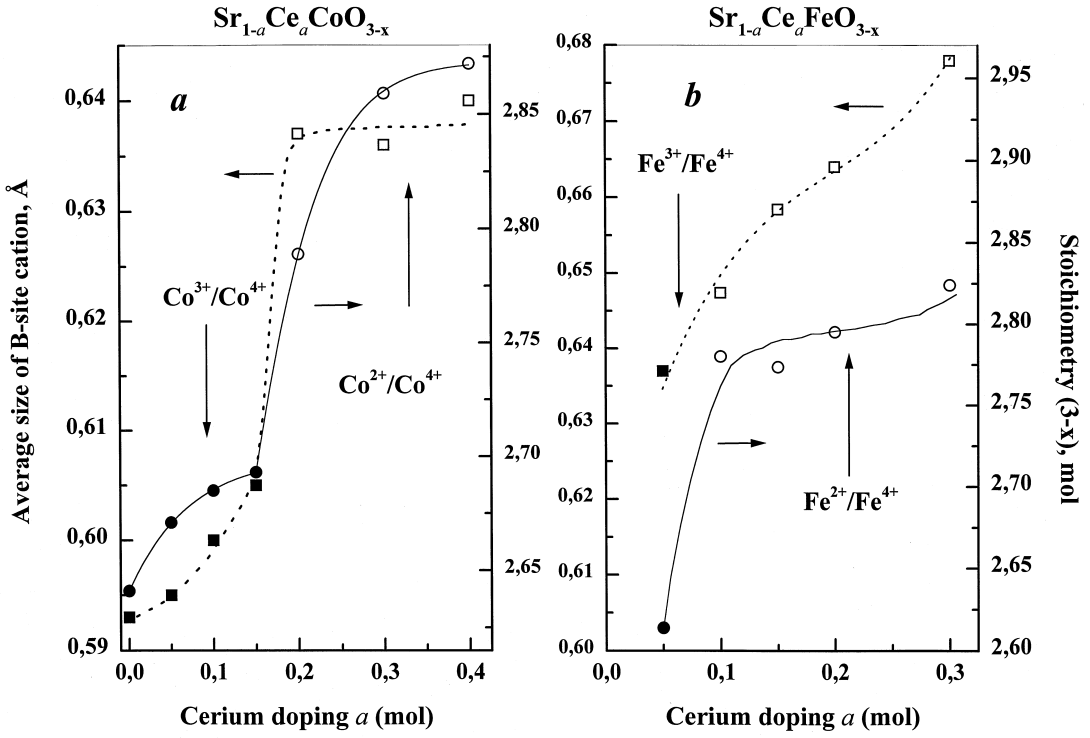

Fig. 2. Average radius of B-site cation □ and oxygen stoichiometry ○ versus cerium doping on A-site in strontium cobaltite (**a**) and strontium ferrate (**b**). Open symbols M^{2+}/M^{4+}, full symbols M^{3+}/M^{4+}.

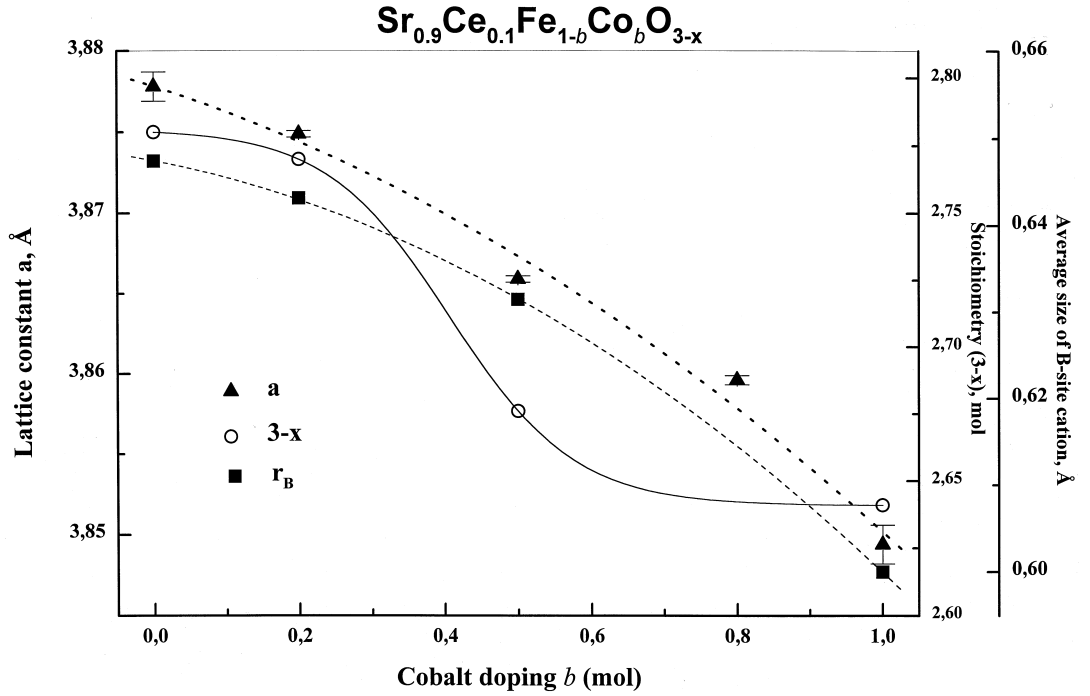

Fig. 3. Lattice constant a ▲, average radius of B-site cation ■ and oxygen stoichiometry ○ versus cobalt doping on B-site. B-site cation ratio corresponds to M^{3+}/M^{4+}.

members $Sr_{0.9}Ce_{0.1}CoO_{3-x}$ and $Sr_{0.9}Ce_{0.1}FeO_{3-x}$. It must be noted, that the solubility limit of cerium depends additionally on the iron/cobalt ratio on the B-site. Higher iron content reduced the cerium solubility (see Table 1). As demonstrated in Fig. 3, the x values increase with increasing cobalt content, they range from 0.275 (for $b=0$) to 0.65 (for $b=1$).

From SEC data, the relation between $(3-x)$ and P_{O2} for $Sr_{0.95}Ce_{0.05}Fe_{0.8}Co_{0.2}O_{3-x}$ at different temperatures is shown in Fig. 4a. Room temperature XRD analysis

Table 1
Lattice parameters and unit cell volumes of the system $Sr_{1-a}Ce_aFe_{1-b}Co_bO_{3-x}$

a (Mol)	b (Mol)	Sintering T (°C)	Lattice parameter a (Å)	Unit cell vol. (Å^3)
0.1	0	1350	3.8778	58.31
0.1	0.2	1350	3.8749	58.58
0.1	0.5	1250	3.8659	57.78
0.1	0.8	1250	3.8596	57.49
0.1	1.0	1250	3.8494	57.04
0.05	0.2	1350	3.8687	57.90
0.15	0.2	1350	3.8800	58.41
0.2[a]	0.2	1350	3.8845	58.61
0.05	0.5	1250	3.8548	57.28
0.15[a]	0.5	1250	3.8626	57.63
0.05	0.8	1250	3.8624	57.62

[a] Trace of second phase (CeO_2).

of this composition after quenching from 800°C at $P_{O2}\sim10^{-10}$ Pa revealed a single phase perovskite-type. The oxygen stoichiometry as function of P_{O2} at 800°C for different compositions is pictured in Fig. 4b. All air-oxidized samples were oxygen deficient. The value of initial oxygen deficiency increases with increasing cobalt content (b) and decreasing ceria content (a). The relative position of the $(3-x)$-vs-P_{O2} curves for compositions with higher Co content shifts to the right compared with the position of the curve for ferrates, suggesting a greater tendency for reduction of the cobaltites. That means ionic compensation becomes more prevalent as Co and Sr content increase. Similar trends were observed in. Refs. 8 and 21. This is in good relation to the thermodynamic data of the pure oxides:[18] Cobalt oxide at 800°C and $P_{O2}<10^{-2}$ Pa is reduced to the 2+ state, at $P_{O2}<10^{-10}$ Pa down to the metallic state, whereas iron oxide at $P_{O2}<10^{-10}$ Pa is reduced to the 2+ state. With increasing temperature and decreasing P_{O2} the oxygen deficiencies x of $Sr_{1-a}Ce_aFe_{1-b}Co_bO_{3-x}$ increase. With increasing cobalt content all compositions were decomposed at the above mentioned conditions into mixtures containing additional phases beside the desired perovskite solid solution. Depending on P_{O2} and temperature the reduction may terminate in the formation of SrO, CeO_2, Fe_2O_3 and CoO or metallic cobalt.

The observed relation of $(3-x)$ to P_{O2} can be divided into three regions: In the highest P_{O2} region the desorption of oxygen from an air-oxidized sample into gases grows considerably with decreasing P_{O2} of the gas. In the region near electronic balance the sample composition doesn't change essentially. In the lowest P_{O2} region the sample again lost oxygen with decreasing P_{O2}. These results agree well with the model of Mizusaki.[23,24]

4.2. Electrical conductivity characteristics

4.2.1. Total electrical conductivity

Results of electrical conductivity measurements on several compositions of $Sr_{1-a}Ce_aFe_{1-b}Co_bO_{3-x}$ in air

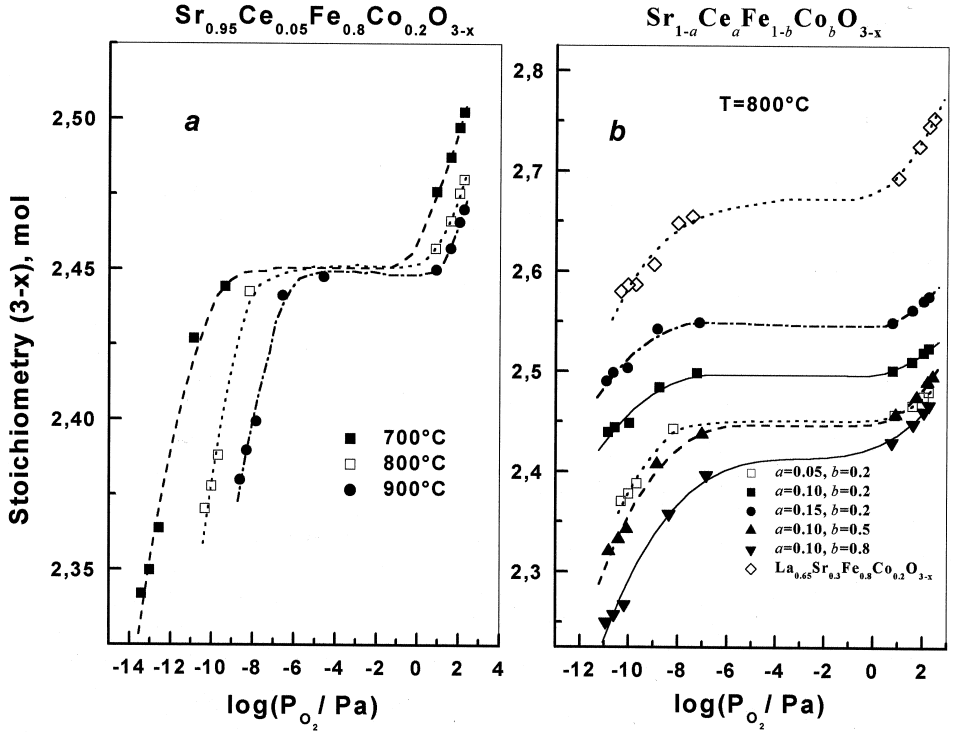

Fig. 4. Oxygen partial pressure dependency of oxygen stoichiometry $(3-x)$ for strontium ferrates/cobaltites: (a) $Sr_{0.95}Ce_{0.05}Fe_{0.8}Co_{0.2}O_{3-x}$; (b) $Sr_{1-a}Ce_aFe_{1-b}Co_bO_{3-x}$, $La_{0.65}Sr_{0.3}Fe_{0.8}Co_{0.2}O_{3-x}$.

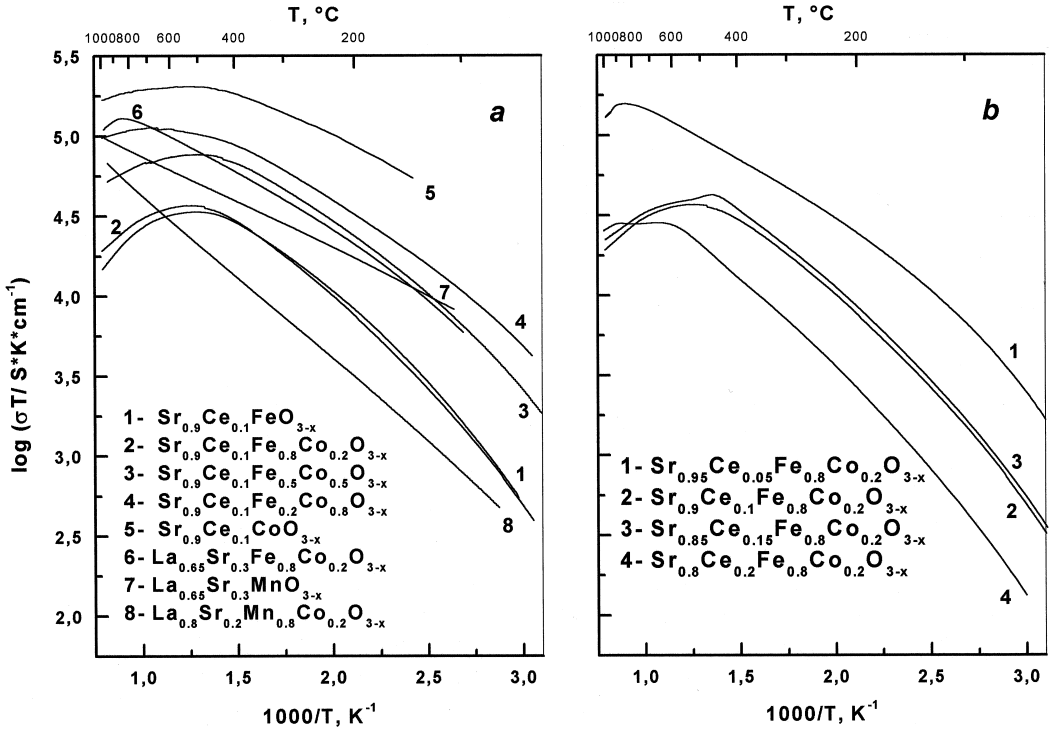

Fig. 5. Electrical conductivity as log σT versus $1000/T$ of $Sr_{1-a}Ce_aFe_{1-b}Co_bO_{3-x}$ in air. (a) for different Fe/Co ratios, compared to $La_{1-a}Sr_aMO_{3-x}$ (M = Fe, Co, Mn); (b) for different Ce concentrations in $Sr_{1-a}Ce_aFe_{0.8}Co_{0.2}O_{3-x}$.

are plotted in Fig. 5. The conductivity of the samples with constant Ce content ($a=0.1$) was enhanced by increasing Co content b (Fig. 5a). The highest values of electrical conductivity (200 S cm^{-1} at 600°C) for samples with $b=0.2$ (Fig. 5b) were observed for the composition of the lowest Ce content: $Sr_{0.95}Ce_{0.05}Fe_{0.8}Co_{0.2}O_{3-x}$. The electrical conductivity decreases rapidly and the activation energy increases with increasing ceria doping. This result is consistent with previous studies on $Sr_{1-a}Ce_aFeO_{3-x}$ and $Sr_{1-a}Ce_aCoO_{3-x}$.[11,12]

The conductivity obtained by d.c. measurements is representative meanly of the electronic part (the ionic transport number in similar compositions is typically less than 1%). All samples show semiconducting behaviour at low temperatures and metallic-like at higher temperatures. If the conduction mechanism in the thermally activated region follows the relation

$$\sigma = A/T \cdot \exp(-E_a/kT) \quad (3)$$

the Arrhenius plots of log σT vs $1000/T$ should be linear (E_a is activation energy, k is Boltzmann constant, T is absolute temperature and A is pre-exponential factor). The E_a values are listed in Table 2 as function of Ce and Co content. It can be seen that for compositions with $b=0.2$ a sharp increase of E_a is noted as Ce concentration increases. The activation energies of cobalt rich compositions are smaller (0.11 eV) than the activation energy of ferrates (0.22 eV).

Decreasing conductivity with increasing temperature may also be interpreted as semiconductor-like conductivity, caused by decreasing concentration of electronic defects with increasing temperature.[8,25] The decrease in conductivity at high temperatures occurs approximately in the same temperature region in which a loss of lattice oxygen takes place related to decreasing concentration of electron holes. It follows from the oxygen nonstoichiometry data, at increasing temperature with the loss of oxygen the concentration of M^{4+}-ions decreases according to:

$$2M_M^* + O_O{}^x \Rightarrow V_O^{**} + 2M_M{}^x + 1/2\ O_2 \quad (4)$$

In the compositions investigated in this work, the observed transition of semiconducting to metallic-like

Table 2
Experimental conditions and calculated activation energies of the total electrical and ionic conductivities of $Sr_{1-a}Ce_aFe_{1-b}Co_bO_{3-x}$

a (Mol)	b (Mol)	E_a of σ total		E_a of σ_{ion}	
		T-range, °C	E_a, eV	T-range, °C	E_a, eV
0.1	0	80–380	0.22	700–1000	0.87
0.1	0.2	80–420	0.21	–	–
0.1	0.5	80–380	0.18	–	–
0.1	0.8	80–380	0.16	–	–
0.1	1.0	140–400	0.11	700–1000	0.82
0.05	0.2	160–760	0.14	700–1000	0.73
0.15	0.2	80–440	0.22	750–1000	1.00
0.20	0.2	100–550	0.23	750–1000	0.46

behaviour can not be related to a structure change as observed[25] for $La_{1-a}Sr_aCoO_{3-x}$ at $a \leqslant 0.2$.

The dependence of the electrical conductivity on oxygen partial pressures for compositions $Sr_{1-a}Ce_aFe_{1-b}Co_bO_{3-x}$ ($b < 0.2$) at 800°C is pictured in Fig. 6. The conductivity increases with P_{O2} exhibiting p-type conductivity at higher oxygen pressures. For cobalt rich samples (Fig. 6a) the slope of $m = d(\log(\sigma))/d(\log(P_{O2}))$ is relatively small ($m = 1/7$–$1/10$) and depends on temperature, indicating a defect structure which cannot be described by a simple defect model. Compositions with Co content $b > 0.2$ were decomposed at $P_{O2} < 10^{-5}$ Pa as described above, the conductivity represents the values of mixtures of some phases. The influence of ceria concentration at $b = 0.2$ is pictured in Fig. 6b. The slope of p-type conduction approaches the predicted value ($m = 1/6$–$1/4$) much better for the iron rich compositions $b > 0.2$ The values of the $\sigma_n = \sigma_p$ range from 0.07 to 0.3 S*cm^{-1}. At reducing conditions ($P_{O2} < 10^{-7}$ Pa) *n*-type conduction appears. The prefered cathode material $La_{0.65}Sr_{0.3}MnO_{3-x}$ shows considerably different conduction behaviour, whereas the $La_{0.65}Sr_{0.3}Fe_{0.8}Co_{0.2}O_{3-x}$ has a conduction behaviour very similar to the $Sr_{1-a}Ce_aFe_{1-b}Co_bO_{3-x}$ compositions (Fig. 6a).

4.2.2. Oxygen diffusion

From permeation results the specific permeation flux *j*, chemical diffusion coefficient of oxygen D^*_O and ionic conductivity σ were calculated (Figs. 7 and 8), assuming a bulk diffusion-controlled flux[26] rather than surface exchange kinetics. This assumption appears to be valid, because the thicknesses of the samples (> 1 mm) were considerably greater than the "characteristic thicknesses" reported in Ref. 28. Another indication for a bulk-controlled flux was the dependency of the permeation flux (approximately inversely proportional) on the pellet thickness.

In the $Sr_{1-a}Ce_aFe_{1-b}Co_bO_{3-x}$ compositions, the oxygen flux increased with decreasing ceria content (Fig. 7, excluding the two-phase composition with 0.2 Ce). This result is consistent with the oxygen nonstoichiometry data, which show a decrease in oxygen deficiency with increasing ceria content. The permeation flux *j* increased with increasing temperature, attributed to an increase of both mobility (thermoactivated process) and concentration of lattice oxygen vacancies. A change in the slope of current density versus reciprocal temperature at about 750°C was observed for the composition with higher cerium content ($a = 0.15$). A similar change was observed by Kruidhof et al.[29] for $SrCo_{0.8}M_{0.2}O_{3-x}$ (with M = Cr, Fe, Cu) and Qiu et al.[30] for $SrCo_{0.8}Fe_{0.2}O_{3-x}$. It was related to the order-disorder transition of oxygen vacancies during the brownmillerite phase transition. In contrast to the $SrCo_{0.8}M_{0.2}O_{3-x}$ the X-ray analysis of the $Sr_{1-a}Ce_aFe_{1-b}Co_bO_{3-x}$ compositions show simple cubic symmetry (see above). Therefore, the change in activation energy observed in this work, might be related rather to transition in oxygen exchange to bulk diffusion limitation at lower temperatures.

Activation energies for ionic conductivity are shown in Table 2. The energies in magnitude are similar to that reported for $La_{1-a}Sr_aFe_{1-b}Co_bO_{3-x}$[7,27] and ranges

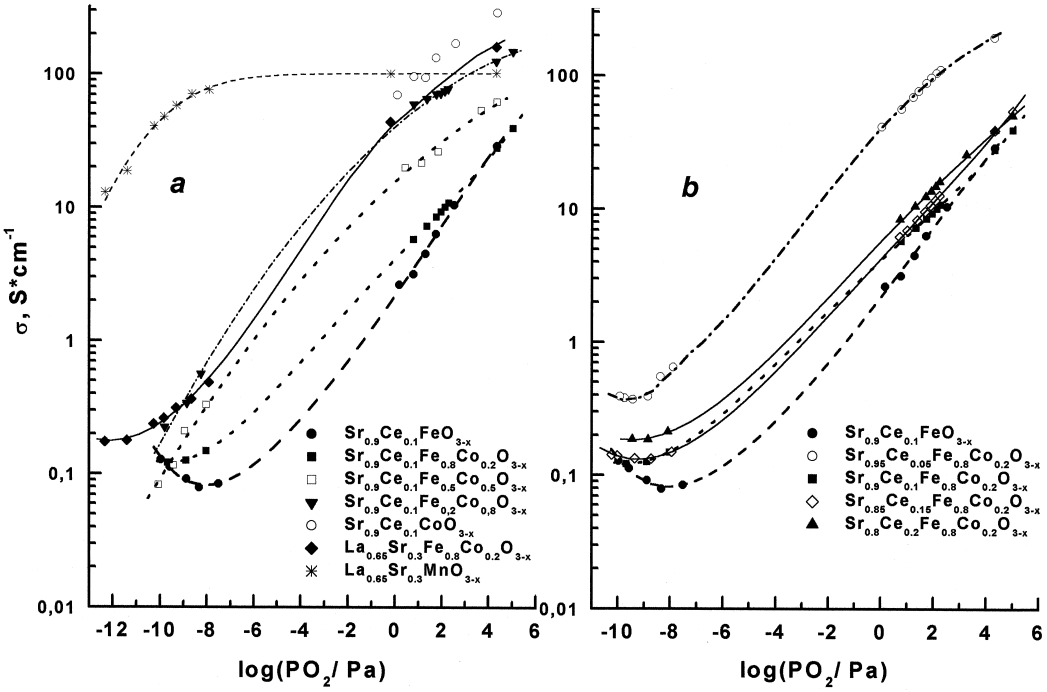

Fig. 6. Electrical conductivity of $Sr_{1-a}Ce_aFe_{1-b}Co_bO_{3-x}$ versus oxygen partial pressure at 800°C (a) dependency on Fe content at constant Ce. For comparison: $La_{0.65}Sr_{0.3}Fe_{0.8}Co_{0.2}O_{3-x}$, $La_{0.65}Sr_{0.3}MnO_{3-x}$; (b) dependency on Ce content at constant Fe.

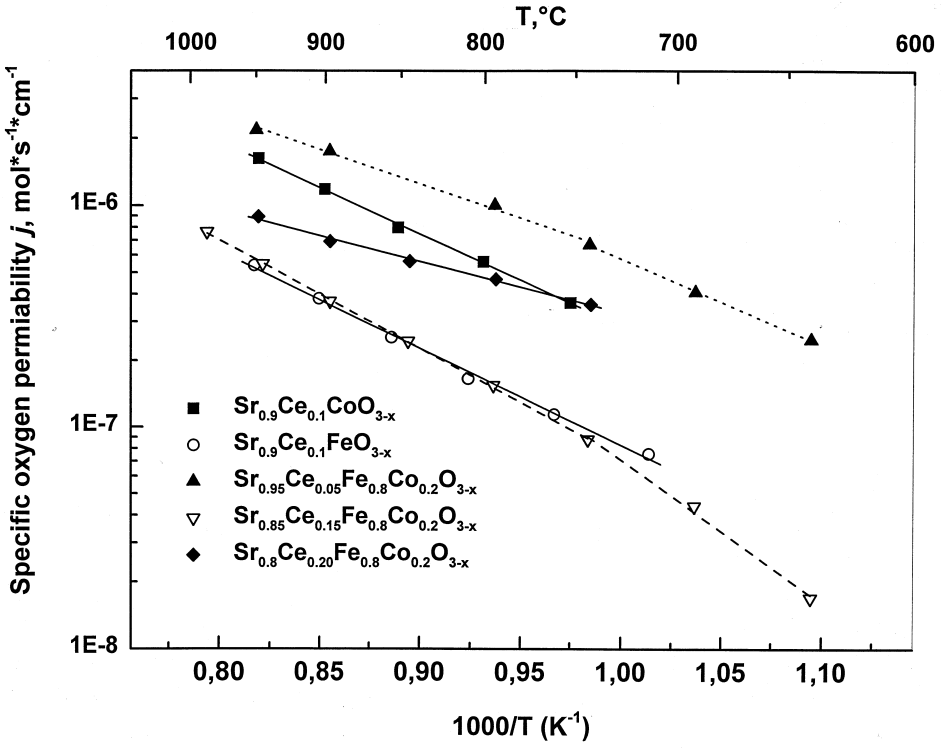

Fig. 7. Specific oxygen permeability, normalized to 1 cm thickness. Oxygen gradient: air/argon + O_2 (70–80 Pa).

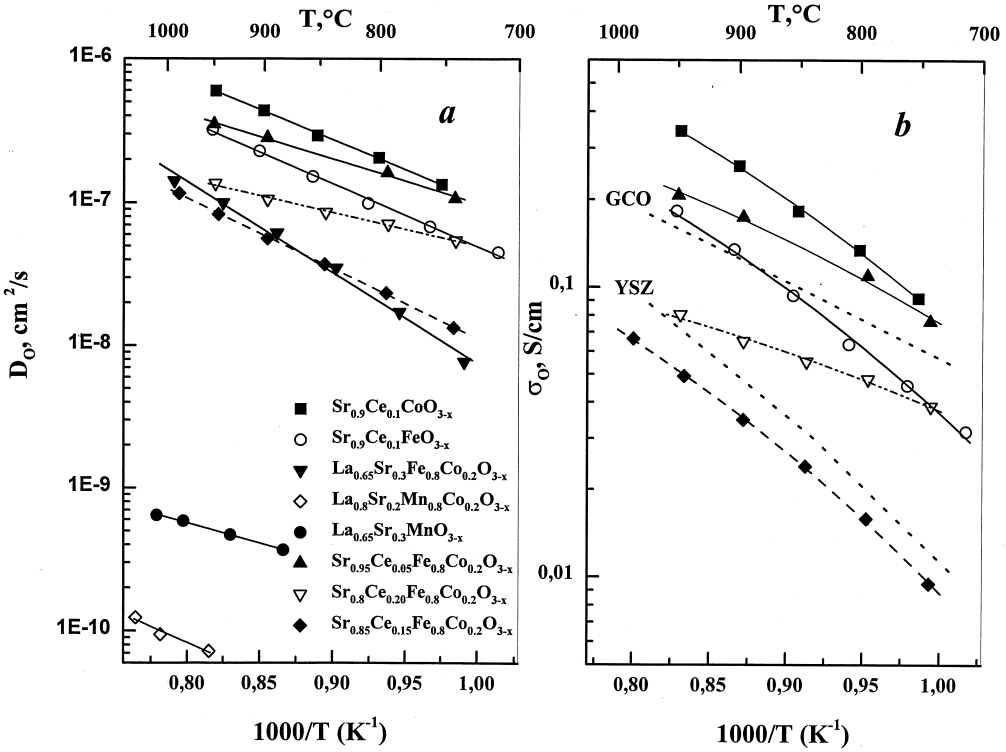

Fig. 8. Results calculated from oxygen permeation measurements; (a) Oxygen chemical diffusion coefficient versus reciprocal temperature; (b) Oxygen ionic conductivity versus reciprocal temperature.

between 0.46 and 1.0 eV. The lowest value for E_a was observed for the heavy ceria doped $Sr_{0.8}Ce_{0.2}Fe_{0.8}Co_{0.2}O_{3-x}$ composition. This might be explained by the presence of CeO_2 as a second phase. REM investigations of $Sr_{1-a}Ce_aFeO_{3-x}$ showed,[12] that in this composite ceria accumulates at the grain boundaries. The samples investigated exhibit D_O values (Fig. 8) of the order 10^{-7}–10^{-8} cm^2 s^{-1} between 1000 and 800°C respectively,

i.e. exceeding the values of manganites by 2 or 3 orders of magnitude. The ionic conductivity values (Fig. 8) of all $Sr_{1-a}Ce_aFe_{1-b}Co_bO_{3-x}$ compositions are higher than that of YSZ and for the $Ce < 0.05$ compositions higher than that of Gd doped ceria.

5. Conclusions

The different behaviour of the lattice parameters *a* of strontium cobaltites (decreasing) and strontium ferrates (increasing) after doping with cerium is explained on the basis of the mean ionic radii of the B-site cations, depending on their oxidation state as calculated from experimentally determined oxygen stoichiometry. The oxygen deficiencies increase with decreasing P_{O2} in the argon/O_2 region as well as in the $Ar/H_2/H_2O$ region. The oxygen deficiencies increase with increasing cobalt content (*b*) and decreasing ceria content (*a*). In compositions with higher Co content additional phases as SrO, CeO_2, Fe_2O_3 and CoO or metallic cobalt occur below 10^{-10} Pa resulting from decomposition.

At constant ceria content the total conductivity of the samples was enhanced with increasing Co content. The highest values of electrical conductivity (200 S cm^{-1} at 600°C; $E_a = 0.14$ eV) were observed for the composition of the lowest Ce content: $Sr_{0.95}Ce_{0.05}Fe_{0.8}Co_{0.2}O_{3-x}$. The electrical conductivity decreases and the activation energy increases with increasing ceria doping. In the temperature range 400–800°C a transition of semiconducting to metallic like behaviour is observed. The semiconduction is of p-type, with a change to n-type in samples of higher iron content at reducing conditions.

The bulk diffusion-controlled flux increased with decreasing ceria content, resulting ionic conductivities exceed that of YSZ and for the $Ce \leqslant 0.05$ compositions that of Gd doped ceria.

Acknowledgements

This work was sponsored by Deutsche Forschungsgemeinschaft, Bonn.

References

1. Steele, B. C. H., Oxygen transport and exchange in oxide ceramics. *J. Power Sources*, 1994, **49**, 1–14.
2. Sekido, S., Tachibani, H., Yamamura, Y. and Kambara, T., Electric-ionic conductivity in perovskite-type oxides $Sr_xLa_{1-x}Co_{1-y}Fe_yO_{3-\delta}$. *Solid State Ionics*, 1990, **37**, 253–259.
3. Kharton, V. V., Naumovich, E. N., Nikolaev, A. V. and Samokhval, V. V., Development of mixed conductive materials for high-temperature electrochemial oxygen membranes. In *Proc. 17th Risoe Int. Symp., High-Temperature Electrochemistry: Ceramics and Metals*, ed. F. W. Poulsen, N. Bonanos and S.et al. Linderoth. Roskilde, Denmark, 1996, pp. 301–306.
4. Kharton, V. V., Naumovich, E. N., Vecher, A. A. and Nikolaev, A. V., Oxide ion conduction in solid solutions $Ln_{1-x}Sr_xCoO_{3-\delta}$ (Ln = La, Pr, Nd). *J. Solid State Chemistry*, 1995, **120**, 128–136.
5. De Souza, R. A. and Kilner, J. A., Oxygen transport in $La_{1-x}Sr_xMn_{1-y}Co_yO_{3+\delta}$ perovskites, Part I. Oxygen tracer diffusion. *Solid State Ionics*, 1998, **106**, 175–187.
6. Figueiredo, F. M., Marques, F. M. B. and Frade, J. R., Electrochemical permeability of $La_{1-x}Sr_xCoO_{3-\delta}$ materials. *Solid State Ionics*, 1998, **111**, 273–281.
7. Teraoka, Y., Zhang, H., Okamoto, K. and Yamazoe, N., Mixed ionic-electronic conductivity of $La_{1-x}Sr_xCo_{1-y}Fe_yO_{3-\delta}$, perovskite-type oxides. *Mater. Res. Bull.*, 1988, **23**, 51–58.
8. Stevenson, J. W., Armstrong, T. R., Carneim, R. D., Pederson, L. R. and Weber, W. J., Electrochemical properties of mixed conducting perovskites $La_{1-x}M_xCo_{1-y}Fe_yO_{3-\delta}$ (M = Sr, Ba, Ca). *J. Electrochem. Soc.*, 1996, **143**, 2722–2729.
9. tenElshof, J. E., Langhorst, M. H. R. and Bouwmeester, H. J. M., Oxygen exchange and diffusion coefficients of strontium doped lanthanum ferrites by electrical conductivity relaxation. *J. Electrochem. Soc.*, 1997, **144**, 1060–1067.
10. Zipprich, W., Waschilewski, S., Rocholl, F. and Wiemhöfer, H.-D., Improved preparation of $La_{1-x}Me_xCoO_{3-\delta}$ (Me = Sr, Ca) and analysis of oxide ion conductivity with ion conducting microcontacts. *Solid State Ionics*, 1997, **101–103**, 1015–1023.
11. Trofimenko, N. E., Ullmann, H., Paulsen, J. and Müller, R., Structure, oxygen stoichiometry and electrical conductivity in the system Sr-Ce-Co-O. *Solid State Ionics*, 1997, **99**, 183–191.
12. Trofimenko, N. E., Paulsen, J., Ullmann, H. and Müller, R., Structure, oxygen stoichiometry and electrical conductivity in the system Sr-Ce-Fe-O. *Solid State Ionics*, 1997, **100**, 201–214.
13. Ullmann, H. and Trofimenko, N., Composition, structure and transport properties of perovskite-type oxides. *Solid State Ionics*, 1999, **119**, 1–8.
14. Ullmann, H., Trofimenko, N., Naoumidis, A. and Stöver, D., Ionic/electronic mixed conduction relations in perovskite- type oxides by defect structure. *J. Eur. Ceram. Soc.*, 1999, **19**, 791–796.
15. Vashook, V. V., Zinkevich, M. V., Ullmann, H., Paulsen, J., Trofimenko, N. and Teske, K., Oxygen non-stoichiometry and electrical conductivity of the binary strontium cobalt oxide $SrCoO_x$. *Solid State Ionics*, 1997, **99**, 23–32.
16. Shannon, R. D., Revised effective ionic radii and systematic studies of interatomic distances in halides and chalcogenides. *Acta Cryst.*, 1976, **A32**, 751–767.
17. van Roosmalen, J. A. M. and Cordfunke, E. H. P., A new defect model to describe the oxygen deficiency in perovskite-type oxides. *J. Solid State Chemistry*, 1991, **93**, 212–219.
18. Knacke, O. Kubaschewski, O. Hesselmann, K. *Thermochemical Properties of Inorganic Substances*, 2nd. Ed. Springer-Verlag, Berlin 1991, Vol.I.
19. Tai, L.-W., Nasrallah, M., Anderson, H., Sparlin, D. and Sehlin, S., Structure and electrical properties of $La_{1-x}Sr_xCo_{1-y}Fe_yO_3$. Part 1. The system $La_{0.8}Sr_{0.2}Co_{1-y}Fe_yO_3$. *Solid State Ionics*, 1995, **76**, 259–271273–283.
20. Jonker, G., Magnetic and semiconducting properties of perovskites containing manganese and cobalt. *J. Appl. Phys.*, 1966, **37**, 1424–1430.
21. Kostogloudis, G.Ch., Fertis, P. and Ftikos, Ch., Electronic conductivity in the $Pr_{1-x}Sr_xCo_{1-y}Mn_yO_{3-\delta}$ system. *Solid State Ionics*, 1999, **118**, 241–249.
22. Teske, K., Ullmann, H. and Trofimenko, N., Thermal analysis of transition metal and rare earth oxide systems — gas interaction by a solid electrolyte based coulometric technique. *J. Thermal Analysis*, 1997, **49**, 1211–1220.
23. Mizusaki, J., Yoshihiro, M., Yamauchi, S. and Fueki, K., Nonstoichiometry and defect structure of the perovskite-type oxides $La_{1-x}Sr_xFeO_{3-\delta}$. *J. Solid State Chem.*, 1985, **58**, 257–266.
24. Mizusaki, J., Mima, Y., Yamauchi, S., Fueki, K. and Tagawa,

H., Nonstoichiometry of the perovskite-type oxides $La_{1-x}Sr_xCoO_{3-\delta}$. *J. Solid State Chem.*, 1989, **80**, 102–111.
25. Mineshige, A., Inaba, M., Yao, T., Ogumi, Z., Kikuchi, K. and Kawase, M., Crystal structure and metal-insulator transition of $La_{1-x}Sr_xCoO_{3-\delta}$. *J. Solid State Chem.*, 1996, **121**, 423.
26. Paulsen, J.M. Thermodynamics, oxygen stoichiometric effects and transport properties of ceramic materials in the system Sr-Ce-M-O (M = Co,Fe), Ph.D. thesis, Technical University Dresden, 1998.
27. Chen, C., Nasrallah, M., Anderson, H. and Alim, M., Immitance response of $La_{0.6}Sr_{0.4}Co_{0.2}Fe_{0.8}O_3$ based electrochemical cells. *Am. Ceram. Soc. Bull.*, 1995, **142**, 491–496.
28. Bouwmeester, H. J. M. and Burggraaf, A. J., Dense ceramic membranes. In *The CRC Handbook of Solid State Electrochemistry*, ed. P. J. Gellings and H. J. Bouwmeester. CRC Press, New York, 1997, pp. 481–553.
29. Kruidhof, H., Bouwmeester, H. J. M., van Doorn, R. H. E. and Burggraaf, A. J., Influence of order-disorder transitions on oxygen permeability through selected nonstoichiometric perovskite-type oxides. *Solid State Ionics*, 1993, **63–65**, 816–822.
30. Qiu, L., Lee, T. H., Liu, L.-M., Yang, Y. L. and Jacobson, A. J., Oxygen permeation studies of $SrCo_{0.8}Fe_{0.2}O_{3-\delta}$. *Solid State Ionics*, 1995, **76**, 321–329.